HHS Public Access

Author manuscript

*Leukemia*. Author manuscript; available in PMC 2017 January 06.

Published in final edited form as:

*Leukemia*. 2017 January ; 31(1): 151–158. doi:10.1038/leu.2016.166.

# Patient-derived xenotransplants can recapitulate the genetic driver landscape of acute leukemias

**Kai Wang**[1,¶,§], **Marta Sanchez-Martin**[2,§], **Xujun Wang**[3,♭,§], **Kristina M. Knapp**[3], **Richard Koche**[3], **Ly Vu**[3], **Michelle K. Nahas**[1], **Jie He**[1], **Michael Hadler**[1], **Eytan M Stein**[3], **Martin S. Tallman**[3], **Amy L Donahue**[1], **Garrett M Frampton**[1], **Doron Lipson**[1], **Steven Roels**[1], **Philip J. Stephens**[1], **Eric M Sanford**[1], **Tim Brennan**[1], **Geoff A. Otto**[1], **Roman Yelensky**[1], **Vincent A. Miller**[1], **Michael G. Kharas**[3], **Ross L. Levine**[3], **Adolfo Ferrando**[2], **Scott A. Armstrong**[3], and **Andrei V. Krivtsov**[3]

[1]Foundation Medicine, Inc. 150 Second St, Cambridge, MA 02141

[2]Institute for Cancer Genetics Columbia University, 1130 St Nicholas Ave, New York, NY 10032

[3]Memorial Sloan Kettering Cancer Center, 1275 York Avenue, New York, NY 10065

## Abstract

Genomic studies have identified recurrent somatic mutations in acute leukemias. However, current murine models do not sufficiently encompass the genomic complexity of human leukemias. To develop pre-clinical models, we transplanted 160 samples from patients with acute leukemia (AML, MLL, B-ALL and T-ALL) into immunodeficient mice. Of these, 119 engrafted with expected immunophenotype. Targeted sequencing of 374 genes and 265 frequently rearranged RNAs detected recurrent and novel genetic lesions in 48 paired primary tumor (PT) and patient-derived xenotransplant (PDX) samples. Overall, the frequencies of 274 somatic variant alleles correlated between PT and PDX samples, although the data were highly variable for variant alleles present at 0-10%. 17% of variant alleles were detected in either PT or PDX samples only. Based on variant allele frequency changes, 24 PT-PDX pairs were classified as concordant while the other 24 pairs showed various degree of clonal discordance. There was no correlation of clonal concordance with clinical parameters of diseases. Significantly more bone marrow samples than peripheral blood samples engrafted discordantly. These data demonstrate the utility of developing PDX banks for modeling human leukemia, and emphasize the importance of genomic profiling of PDX and patient samples to ensure concordance before performing mechanistic or therapeutic studies.



Corresponding author: Andrei V. Krivtsov, PhD, Assistant Lab Member, Memorial Sloan-Kettering Cancer Center, Rockefeller Research Building, RRL-417E, 430 East 67th Street, New York, NY 10065, krivtsoa@mskcc.org, Tel. 646 888 3589, Fax. 646 888 3406.

¶current address: Department of Pathology & Cancer Research Institute, Zhejiang Cancer Hospital, Hangzhou, 310022, China

♭current address: Cornell University, 1300 York Ave, New York, NY 10065

§these authors equally contributed to this work.

**Conflict of Interest**: KW, MKN, JH, ALD, GMF, DL, SR, PJS, EMS, TB, GAO, RY, VAM are employees and equity holders, RLL is a consultant for Foundation Medicine, Inc.

## Introduction

Acute myeloid and lymphoid leukemias are heterogeneous diseases with subsets having dismal prognosis[1]. Successful development of novel targeted therapies critically depends on the availability of genetically annotated pre-clinical animal models, which may be informative for initiation of clinical trials and understanding resistance to novel targeted therapeutics. Currently, the choices for pre-clinical animal models are: genetically engineered mouse models (GEMMs) of human leukemias or patient-derived xenotransplant (PDX) models. Advantages of GEMMs include their defined genetics and scalability. Unfortunately, GEMMs do not cover much of the spectra of genetic lesions that occur in patients[2]. The potential advantage of PDX models is the genetic diversity that is found in patients and that is likely to be important for preclinical assessment of therapies targeting specific genetic lesions. PDX models are widely used for studying the biology of diseases and testing potential compounds, however it remains unclear the extent to which PDXs faithfully maintain the genetic and genomic complexity seen in primary patient samples[3-6].

Large-scale sequencing of genomes and whole exomes in samples from newly diagnosed and relapsed leukemia patients has demonstrated recurrent genetic aberrations that are, in some cases, specific for disease lineage. Sequencing has also revealed that, in some cases, the mutant alleles and their frequencies differ between samples from newly diagnosed and relapsed acute leukemia patients[7]. These findings support the concept of genetic drift and that tumorigenesis is a continuous process in which mutations are acquired sequentially. At any point in the process, a founding and minor clone(s) may coexist and the latter may eventually become dominant. Therefore, acute leukemia may be initiated as a monoclonal disease and become polyclonal after acquiring additional genetic lesions[8-10]. Recently, the usefulness of PDX models for pre-clinical assessment has been questioned because of the clonal selection that occurs after transplantation of PT samples into immunodeficient mice[11-13]. The aims of this study were: 1) to establish a collection of engraftable and genomically annotated patient samples; 2) to assess which leukemia relevant mutant alleles engraft in mice with frequency similar to that observed in PT samples.

## Materials and Methods

### Patient samples and transplantations

Acute myeloid leukemia (AML) and B-cell acute lymphoblastic leukemia (B-ALL) patient samples were acquired from the Hematologic Oncology Tissue Bank at Memorial Sloan Kettering Cancer Center; T-cell ALL (T-ALL) patient samples were acquired from the ECOG study and Columbia University Hospital under IRB approved protocols. All patients provided written informed consent. Samples were intravenously injected into 1 to 6 (on average 2) irradiated (200 RADs) NSG mice at $10^5$-$10^6$ viable cells per mouse[5].

### Sequencing and detection of genomic variances

Genomic (g) DNA and total RNA were isolated only from unfractionated PT (mixture of hematopoietic and leukemia cells) and PDX samples (mixture of engrafted human and murine cells); germline samples were absent and therefore not analyzed. Adaptor-ligated

sequencing libraries were captured by solution hybridization with two custom bait-sets targeting 374 cancer-related genes, 31 genes frequently rearranged by DNA-seq and 265 genes frequently rearranged by RNA-seq, with the FoundationOne Heme test, sup table 1. All captured libraries were sequenced on HiSeq2500, Illumina[14]. For amplicon-sequencing gDNA was isolated from 7 available and not related PDX samples, selected genomic regions were amplified using microdroplet-PCR followed by illumina sequencing[15]. Excluding PE100 reads that align to mouse genome (mm9) in PDX samples resulted in loss <0.6% reads, which was considered not to affect VAF and therefore disregarded[16].

For detailed description please refer to supplemental methods.

## Results

### Acute leukemia patient samples robustly engraft in NSG mice

We transplanted 160 patient samples, balanced by disease lineage, status and patient age, into NSG mice, sup table 2. Of these, 119 engrafted as assessed by FACS (>0.1% human CD45) in peripheral blood (PB) or bone marrow (BM) or spleen (SP) tissues in at least one mouse with lineage matching classification of patient disease, table 1, sup table 3. Forty-five (80%) AML samples engrafted as $CD45^+CD33^-CD19^-CD3^-$; $CD45^+CD33^+CD19^-CD3^-$ or $CD45^+CD33^+CD19^+CD3^-$ with a median latency of 107 ± 41 days, sup figure 1A. Two AMLs engrafted as $CD45^+CD19^+CD33^-CD3^-$; 1 AML engrafted as $CD45^+CD19^-CD33^-CD3^+$; 6 AML samples produced mixed myeloid ($CD45^+CD33^+$) and T-lymphoid ($CD45^+CD3^+$) grafts. We detected both CD4+ and CD8+ T-cells were engrafting in NSG mice transplanted with AML samples, sup figure 1D. Therefore, subsequent AML samples were subjected to CD3-depletion prior to transplant. Secondary transplantation of 6 PDX AML samples resulted in disease with the same immunophenotype with a latency of 87 ± 35 days. One mixed lineage leukemia (MLL) engrafted as $CD45^+CD33^+CD19^-CD3^-$ within 134 ± 12 days, and 1 MLL engrafted as $CD45^+CD33^-CD19^+CD3^-$ within 72 ± 5 days. 75% of the B-ALLs engrafted within 95 ± 44 days, including 24 B-ALLs engrafted as $CD45^+CD33^-CD19^-CD3^-$ or $CD45^+CD19^+CD33^-CD3^-$ and 1 B-ALL engrafted as $CD45^+CD33^+CD19^+CD3^-$, sup figure 1B. Two B-ALL samples produced $CD45^+CD19^+$ and $CD45^+CD3^+$ grafts. Secondary transplantation of 3 PDX B-ALLs engrafted as $CD45^+CD19^+CD33^-CD3^-$ in all mice within 40 ± 11 days. Similarly, 48 T-ALL samples (69%) engrafted within 50 days, maintaining expression of CD45 and various combinations of additional markers, including CD2, CD3, CD4, and CD7, sup figure 1C. Secondary transplantation of 2 PDX T-ALL samples resulted in engraftment within 29 ± 11 days.

Overall, PDX samples were amplified during engraftment in mice and some retained the patients' disease immunophenotype. In 5 of 10 sequentially available AML and corresponding PDX samples we detected similar distribution patterns of CD34/CD38 labeled populations, which frequently used for assessments of leukemia stem cells, sup figure 2 and sup table 4. Shorter latency in secondary PDX transplants was observed for all lineages of leukemias. No significant difference was apparent in engraftment of PT BM vs. PB or newly diagnosed vs. refractory vs. relapse samples in any disease sub-groups.

### Detection of genetic lesions in acute leukemias

Using the FoundationOne Heme test, we assessed the presence of chromosomal rearrangements (RE), copy number aberrations (CNA), short genomic insertions and deletions (InDel), and substitutions (SNV) in 67 patient samples and 94 PDX samples chosen based on material availability and balanced by disease lineage, sup tables 3, 5, 6. Detected genomic lesions that had either been previously published as recurrent in leukemia from literature or public database COSMIC[17], or were predicted to alter protein function on tumor suppressor genes were designated as somatic variant alleles (SVA); other genomic variants were designated as variants of unknown significance (VUS)[14, 18]. VUS were enriched in SNPs and were used in analyses independently.

We detected sequences corresponding to fusion RNA of known RE in 23 PT samples: *MLL1-AF4* (in 4 samples), *MLL1-AF9* (2), *MLL1-AF10* (1), *MLL1-ELL* (1), *MLL1-ENL* (1), *MLL1-EP300* (1), *MLL1-PTD* (1), *BCR-ABL* (1), *BCL2-IGK* (1), *CRLF2-P2RY8* (2), *ETV6-RUNX1* (2), *PBX1-TCF3* (2), *MYH11-CBFB* (1), and *TAL1* internal rearrangements (1). In 3 B-ALL and 2 T-ALL samples we detected multiple RE. In 3 PT and matched PDX samples, we detected sequences corresponding to likely novel fusion proteins, such as RB1-RCBTB2 (1), PAX5-FLI1 (1) and PAX5-MSI2 (1).

The most frequent SNV, InDel, and CNA detected were: *CDKN2A* (28), *CDKN2B* (22) deletions; *TP53* (12), *FLT3* (SNV and ITD) (11), *NOTCH1* (11), *WT1* (11), *NRAS* (10), *PTEN* (10), *PTPN11* (9), *NPM1c* (7), *JAK1/2/3* (6), *KRAS* (6), *DNMT3A* (6), *IDH1/2* (5), and *ASXL1* (5), table 2 and sup table 6; similarly to previously reported[10, 19]. All mutations detected in PT using clinical tests were also confirmed by FoundationOne Heme[18].

### Variant allele frequencies correlate in PDX and patient samples

To be a faithful pre-clinical model for targeted therapeutics, PDX should to recapitulate the genetic lesions of the original PT samples. In 48 PT-PDX paired groups (16 AML, 1 MLL, 15 B-ALL, 16 T-ALL), with median coverage >500×, we detected 274 SVA and 714 VUS. Twenty-eight (10%) SVA were not detected in PT and 28 were not detected in PDX samples. Population heterogeneity or accuracy of detection or sampling could explain the differences in the genetic markup between the PT and PDX.

SVA frequency (SVAF) and VUS values correlated between PT and PDX samples (Pearson, both $p < 10^{-4}$) without correction for percent-blasts in PT samples. The SVAF mean increased from 0.292 in PT to 0.354 in PDX samples (Wilcoxon, $p < 10^{-4}$), whereas the VUS means in PT and PDX samples were similar at 0.444 and 0.455. These findings indicate that SVAF but not VUS marked the clones were enriched in PDX isolates. To assess the dynamics of the increase in SVAF values in PDX, we binned PT SVAF values into four groups roughly representing: “minor clone mutation” (0-10%); “major clone mutation” (10-30%); “heterozygous mutation” (30-70%); and “homozygous mutation” (70-100%). We then assessed whether PT and PDX SVAF values correlate within these 4 bins. SVAF and VUS values correlated in 10-100% range in PT-PDX pairs, but no correlation was observed in the 0-10% range, figures 1A&B, sup table 7. This finding either suggests that most of the rare clones (SVAF <10%) change their share in the bulk leukemia, or reflects a high

technical standard deviation (SD) of the detection of low frequency events. To assess sensitivity and accuracy of FoundationOne Heme test we sequenced amplicons of 30 genes[15] from 7 PDX samples, which resulted in detection of all 17 SVAF. Plotted SVAF from FoundationOne Heme and 30-gene amplicons demonstrated highly correlated ($R^2$=0.802, $p<10^{-4}$) but not uniform data, suggesting that the SVAF obtained form a single method should be considered to be used with a wider SD, than calculated using the variance and depth-coverage from the single method, figure 1C.

To enumerate the increase of SVAF in PDX samples, we measured a distance deviation (DD) between *expected* SVAF (PDX=PT) and *measured* SVAF values, figure 2A. DD distributions between measured and expected VAF values was significantly larger for somatic than VUS ($D^{K-S}$ = 0.29, $p < 10^{-4}$). Histogram presentation of DD showed that VUS have a monomodal distribution with 91% values <10%, whereas SVAF have a bimodal distribution, with only 68% values in same range; and 28% (vs. 7% for $DD^{VUS}$) in the 15-50% range, black bars represent ranges in figure 2B. This distribution pattern confirms that VUS are less variable and are likely present in all cells of PT samples. Suggesting that SVAF mark the clones that change in frequency relative to the original bulk tumor. To assess what SVAF values are the most variable between PT and PDX samples we subdivided them into 3 groups 0-10%, 10-30%, and 30-100% by PT values. SVAF of the 10-30% group was the most variable 48% in 15-50% DD window, while 0-10 and 30-100% groups showed 17% and 18% DD variability, respectively, figure 2C. Moreover, in SVAF of the 10-30% group, 24 of 53 (45%) values changed ≥2-fold in PDX as compared with PT samples.

Overall, both SVAF and VUS values significantly correlate between PT and PDX samples. SVAF have higher variability between PT and PDX samples, which suggests clonal changes in PDX samples. The most variable SVAF values were in the “minor clone mutation” range (0-10%), likely representing high SD of detection. However, close to half of SVAF marking “major clones” contributes to the observed clonal changes.

## Concordance of leukemia drivers within individual patients and PDX pairs

It has been previously reported that the clonal composition of PDX samples may change after engraftment in non-irradiated immunodeficient recipient mice[11]. We speculated that if genetic mutations instruct clonal selection, the clones must possess at least one genetic variant that provides a competitive advantage over the founding clone in the tumor. Data plotted in figure 2B suggest that SVA are more likely to contribute to clonal discordance (CD), as previously suggested[20]. Scatter plots of SVAF values for individual PT-PDX pairs can be classified into two groups. 1) SVAF cluster around perfect uniformity line or PT and PDX samples are clonally concordant (CC), figure 3A, sup figure 3A and 2) SVAF are randomly scattered or PT and PDX are CD, figure 3B, sup figure 3B. We therefore, quantified CD of PT-PDX samples using two parameters: (1) the same variant alleles are detected in paired PT-PDX samples[21]; (2) a fold change in SVAF between paired PT-PDX samples. First, we assessed CC of PT-PDX using the detection of SVAF≥10% in both PT and PDX samples, since previous publications indicated that an SVAF of <10% has a high false discovery rate (FDR)[11]. One or more SVA were missing in 4 PDX samples, four PT samples, or 7 paired PT-PDX, figure 3C. Second, we measured CD on the basis of a ≥2-fold

change in the values of SVAFs in the 10-90% range. Nineteen PT-PDX pairs had at least one variant allele that changed frequency ≥2-fold, figure 3D. Overall, 24 of 48 PT-PDX pairs were considered CC using 2 criteria: <2-fold change for SVAF and presence of all SVAF>10%, sup table 8.

Concordantly engrafting PT samples did not differ from discordantly engrafting PT samples in latency or engraftment levels in murine BM or SP tissues. There was no correlation between concordance of engraftment and disease lineage, disease status (if all disease lineages were analyzed together), patient age, or future relapse or adverse clinical outcome. Deletions within *CDKN2A/B* loci or known rearrangements did not correlate with CD. At the same time, known RE and *CDKN2A/B* loss appear to be mutually exclusive (Fisher, $p < 10^{-4}$), sup tables 2 and 9.

Nevertheless, 11 of 14 PDX that arose from PT BM samples were CD as compared with only 8 of 26 PDX that arose from PT PB samples (Fisher, $p < 0.05$). PT samples that produced CC PDX on average had an insignificantly higher mean of blast content 72% compared with 61% of samples producing CD PDX. Therefore, it is plausible that the sample tissue and tumor burden may contribute to the observed CD, sup table 8.

## Stable variant alleles in clonally discordant samples

Sequencing of diagnostic (D) and relapsed (R)PT 017 along with 4 PDX samples (017D_PDX15, 017DPDX16, 017D_PDX17, 017R_PDX210), identified that 6 samples carry an *MLL-AF9* translocation, $PTPN11^{G503A}$, and combinations of $ECT2L^{R852Q}$, $NRAS^{G12S}$ and *FLT3-ITD*, figure 4. PT 017D, carried only *MLL-AF9*, $ECT2L^{R852Q}$ and $PTPN11^{G503A}$; 3 PDX showed additional $NRAS^{G12S}$, and 017D_PDX16, 017D_PDX17 showed additional variant alleles of *FLT3-ITD* (all <10%). It is unlikely that the same mutations occurred in 2 or 3 independent mice; more likely, these mutations already existed in 017D under the detection limit. Sequencing of PT 017R detected *MLL-AF9*, $ECT2L^{R852Q}$, $PTPN11^{G503A}$, *FLT3-ITD* and $NRAS^{G12S}$. However, the $VAF^{PTPN11}$ decreased from 23% in 017D to 2% in 017R and the similarly $VAF^{FLT3\text{-}ITD}$ increased from "not detectable" to 14%; $VAF^{NRAS}$ in 017R was 2%, similar to the range detected in 017D_PDX15, 017D_PDX16 and 017D_PDX17.

We conclude that it is likely that this AML sample at diagnosis had at least three sub-clones carrying *MLL-AF9* and $ECT2L^{R852Q}$ and each was uniquely marked with (1) $PTPN11^{G503A}$, (2) *FLT3-ITD* and (3) $NRAS^{G12S}$. In the relapsed sample, the clone (3) marked with $NRAS^{G12S}$ did not change frequency; it was minor and remained the minor clone. The clone (2) marked with *FLT3-ITD* expanded from a minor to a major clone. The clone (1) marked with $PTPN11^{G503A}$ decreased from a major to a minor clone. Although PDX and PT samples demonstrated some variability in SVAF, overall, the PDX samples proportionally represented PT samples. Since *MLL-AF9* and $ECT2L^{R852Q}$ were detected in all samples at similar levels, there is no basis to exclude any of these samples from testing therapeutics targeting either of these mutations. 017D may also be considered for experiments targeting $PTPN11^{G503A}$, and 017R for experiments targeting FLT3-ITD. This observation led us to assess not the clonal concordance of an individual PT-PDX pairs, but rather consistency of engraftment of individual allele across multiple PT-PDX pairs.

### Correlation of allele frequencies of somatic variance between PT and PDX samples

Lastly, we assessed whether variation of SVAF values between PT and PDX samples might be influenced by annotated gene function. We plotted the distribution of DD means for the recurrent (n ≥ 2) 30 genes. We used the mean DD of all SVAFs (12.7%), as a threshold for classification, figure 5A, sup table 10. SVAFs for 18 recurrent genes demonstrated mean DD <12.7% and therefore were considered *similar* between PT and PDX samples, figure 5B, sup figures 4A. These are the mutations in genes that are likely either initiating events in leukemia pathogenesis, such as *DNMT3A*, *PTPN11*, *WT1*, *FBXW7* and *RUNX1*[22-25], or do not influence engraftment in mice. In reviewing a similar group, we found that those whose variant allele values were similar between PT and PDX samples were also present on average in 60% ± 30% of concordant samples, sup table 10. Overall, in the similar group, 6 of 18 genes, such as *RUNX1*, *APC*, *ATM* and *IKZF1*, were exclusively, whereas *FBXW7* and *WT1* were predominantly found in concordant samples.

SVAF for 12 genes demonstrated a mean DD >12.7% and therefore were designated as *divergent* between PT and PDX samples, figure 5C, sup figure 4B, sup table 10. These mutations may occur at later stages of leukemogenesis and may be present in only a fraction of leukemia cells and/or affect engraftment in mice (such as *NPM1*, *MLL2*, *IDH1/2* and *TET2*[22, 26]). In the divergent group, 8 of 12 genes, such as *STAG2*, *MLL2*, *PAX5*, *TET2* and *CEBPA*, were exclusively, whereas *NPM1*, *TP53* and *IDH2* were predominantly found in the discordant samples. Together, alleles whose variances were divergent between PT and PDX samples were present on average in 80 ± 20% of discordant samples, sup table 10. Our data suggest that studies of the divergent alleles in xenotransplant settings will require rigorous genomic testing of PDX samples to ensure the presence of the studied allele at the expected frequency in order to draw any conclusions.

## Discussion

Individual PDX models are currently *de facto* standards in studying the biology of diseases and responses to novel therapeutics, often without extensive genomic characterization[27-29]. We established a resource of 119 PDX samples that can be serially xenotransplanted, 65 of which were annotated for genetic lesions relevant for hematologic malignancies for pre-clinical assessment of targeted therapeutics, tables 1 and 2. Currently, mouse genetic models provide a restricted set of leukemia models. For instance, majority of effort was focused on generating *MLL-fusion*; *IDH1/2*; *FLT3-ITD*; *TET2* and *DNMT3A* mediated AML[2]. While these mutations are present in a significant portion of human leukemias, modeling of human leukemias bearing mutations for instance *WT1*, *PTPN11* or *PHF6* was rather limited[30].

It has been shown that for some B-ALL samples, all genetic variations observed in the PDX samples are already present in the patient sample at low levels[31]. Recent genomic characterization also raises a concern that PDX samples may not truthfully recapitulate clonal hierarchy of AML patient samples and may lead to changes in SVAF of targetable alleles when transplanted into non-irradiated recipient mice[11]. If PDX are a mixture of leukemia and either normal hematopoietic cells of different lineages or pre-leukemic HSC and their progeny, the sequencing readout may identify pre-leukemic VAF at the same frequency as detected in PT samples. These complexities need to be taken into account when

tracking VAF in patient leukemia and PDX models as well as of host mouse strain, which can also influence engraftment of particular hematopoietic lineages[32, 33]. Targeted sequencing coupled with manual curation allows exclusion of false variants that result from low-quality alignment, from low-quality reads, or from belonging to noisy genomic regions[34]. This is one of the benefits of targeted sequencing as manual curation of the whole exome or genome variants is likely to be overly laborious. On the other hand, not having manual curation may yield to variant alleles with unknown relevance.

In our data, SVAF correlated between PT and PDX samples with a modest mean increase in SVAF values in PDX samples. At the same time, 45% of SVAFs whose values were in the 10-30% range in PT samples changed ≥2-fold in PDX samples. Although the variability in the 0-10% range may be attributed to both biological diversity and technical variability, the variation in the 10-30% range is most likely due to CD between PT and PDX samples, figure 2B. Using defined parameters (floor = 10%, ratio ≥2), we classified 24 of 48 PT samples as engrafting clonally concordantly. We observed that in 5 out of 7 (71%) clonally concordant pairs, staining with CD34/CD38 antibodies produced a similar pattern in PT-PDX pairs. All 3 clonally discordant cases produced engraftment with very difference CD34/CD38 patterns. These data could be further used as a rough and quick assessment if PDX recapitulates original PT sample, since in 80% of cases immunophenotypic and genetic assessment of PT-PDX concordance matched, sup table 11.

We found that technical issues such as sample tissue or blast percentage might influence the classification of CC, figures 3 C&D. For instance PT BM samples produced significantly more CD PDX possibly due to contamination of BM cells by stromal and/or fat cells, which may influence VAF. Some differences can be observed between our and previously published studies[11]. Such as we report that 50% of PT samples engraft clonally concordantly. We verified the lineage of the engrafted PDX by FACS and manually curated the variant alleles, which may partially explain some of the observed differences. We believe it is important to control for normal hematopoietic component (particularly T-cell) reconstitution in PDX samples since hematopoietic cells engraft along with leukemia cells and can dilute “minor clone” SVAF while leaving SVAF that occurred in stem cells unchanged[22]. For instance, in five samples, the mutant *DNMT3A* allele was within the 43-51% range. It has been reported that *DNMT3A* mutation is one of the early mutations that marks the pre-leukemia clone. For instance, the VAF for *NPM1*c, which might be acquired after the first mutation, varied in the 14-56% range[22]. Mutations in *TET2* and *IDH2* are believed to be initiating leukemogenic events in leukemia[22, 31]. Nevertheless, we observed significant variation in engraftment of *IDH2* and *TET2* alleles post engraftment. Currently, IDH1/2 inhibitors are being studies in clinical trials[35]. We also detected $IDH2^{R140Q/W}$ mutation frequency in 4-26% range in 3 PT samples, which does not support that that these mutations are initiatin, sup table 6. Our data suggest that using PDX models for studying *IDH1/2* or *TET2* mutations might be risky and ought to include testing SVAF in all the mice.

In 18 of 30 genes, we observed *similar* SVAF values in PT and PDX samples; these include likely founding mutations in *DNMT3A*, *RUNX1* and *NOTCH*. At the same time, the SVAF in 12 genes have divergent values between PT and PDX samples. This might happen

because these mutations are sub-clonal and influence engraftment in mice. Therefore, we conclude that PDX models will be useful for studying genomic alterations that are either known founding mutations in leukemia or do not influence engraftment. The use of PDX samples might be less informative for alleles such as *PTEN* or *TP53*, which engraft at very different frequencies in mice as compared to the PT samples. It is important to note, if SVAF is consistently increased in frequency, such as *NPM1c*, the PDX models might still be useful for studying the allele but this characteristic needs to be considered in any experimental interpretation.

## Supplementary Material

Refer to Web version on PubMed Central for supplementary material.

## Acknowledgments

We thank Chun-Wei (David) Chen, Omar Abdel-Wahab, and Alex Kentsis for critical discussion of the manuscript, Barb Every for editor help. Research funding was provided by the Kleberg Foundation and R01 CA176745/CA/NCI NIH.

## References

1. ADAM. Acute myeloid leukemia. ADAM Medical Encyclopedia. 2014 May 29.
2. Walrath JC, Hawes JJ, Van Dyke T, Reilly KM. Genetically engineered mouse models in cancer research. Advances in cancer research. 2010; 106:113–164. [PubMed: 20399958]
3. Scott CL, Becker MA, Haluska P, Samimi G. Patient-derived xenograft models to improve targeted therapy in epithelial ovarian cancer treatment. Frontiers in oncology. 2013; 3:295. [PubMed: 24363999]
4. Malaise M, Neumeier M, Botteron C, Dohner K, Reinhardt D, Schlegelberger B, et al. Stable and reproducible engraftment of primary adult and pediatric acute myeloid leukemia in NSG mice. Leukemia. 2011 Oct; 25(10):1635–1639. [PubMed: 21647161]
5. Sanchez PV, Perry RL, Sarry JE, Perl AE, Murphy K, Swider CR, et al. A robust xenotransplantation model for acute myeloid leukemia. Leukemia. 2009 Nov; 23(11):2109–2117. [PubMed: 19626050]
6. Wunderlich M, Mizukawa B, Chou FS, Sexton C, Shrestha M, Saunthararajah Y, et al. AML cells are differentially sensitive to chemotherapy treatment in a human xenograft model. Blood. 2013 Mar 21; 121(12):e90–97. [PubMed: 23349390]
7. Ma X, Edmonson M, Yergeau D, Muzny DM, Hampton OA, Rusch M, et al. Rise and fall of subclones from diagnosis to relapse in pediatric B-acute lymphoblastic leukaemia. Nat Commun. 2015; 6:6604. [PubMed: 25790293]
8. Notta F, Mullighan CG, Wang JC, Poeppl A, Doulatov S, Phillips LA, et al. Evolution of human BCR-ABL1 lymphoblastic leukaemia-initiating cells. Nature. 2011 Jan 20; 469(7330):362–367. [PubMed: 21248843]
9. Zhang J, Ding L, Holmfeldt L, Wu G, Heatley SL, Payne-Turner D, et al. The genetic basis of early T-cell precursor acute lymphoblastic leukaemia. Nature. 2012 Jan 12; 481(7380):157–163. [PubMed: 22237106]
10. Welch JS, Ley TJ, Link DC, Miller CA, Larson DE, Koboldt DC, et al. The origin and evolution of mutations in acute myeloid leukemia. Cell. 2012 Jul 20; 150(2):264–278. [PubMed: 22817890]
11. Klco JM, Spencer DH, Miller CA, Griffith M, Lamprecht TL, O'Laughlin M, et al. Functional heterogeneity of genetically defined subclones in acute myeloid leukemia. Cancer cell. 2014 Mar 17; 25(3):379–392. [PubMed: 24613412]
12. Aparicio S, Hidalgo M, Kung AL. Examining the utility of patient-derived xenograft mouse models. Nature reviews Cancer. 2015 May; 15(5):311–316.

13. Vick B, Rothenberg M, Sandhofer N, Carlet M, Finkenzeller C, Krupka C, et al. An advanced preclinical mouse model for acute myeloid leukemia using patients' cells of various genetic subgroups and in vivo bioluminescence imaging. PloS one. 2015; 10(3):e0120925. [PubMed: 25793878]
14. Frampton GM, Fichtenholtz A, Otto GA, Wang K, Downing SR, He J, et al. Development and validation of a clinical cancer genomic profiling test based on massively parallel DNA sequencing. Nature biotechnology. 2013 Nov; 31(11):1023–1031.
15. Cheng DT, Cheng J, Mitchell TN, Syed A, Zehir A, Mensah NY, et al. Detection of mutations in myeloid malignancies through paired-sample analysis of microdroplet-PCR deep sequencing data. J Mol Diagn. 2014 Sep; 16(5):504–518. [PubMed: 25017477]
16. Li S, Shen D, Shao J, Crowder R, Liu W, Prat A, et al. Endocrine-therapy-resistant ESR1 variants revealed by genomic characterization of breast-cancer-derived xenografts. Cell Rep. 2013 Sep 26; 4(6):1116–1130. [PubMed: 24055055]
17. Forbes SA, Beare D, Gunasekaran P, Leung K, Bindal N, Boutselakis H, et al. COSMIC: exploring the world's knowledge of somatic mutations in human cancer. Nucleic Acids Res. 2015 Jan; 43(Database issue):D805–811. [PubMed: 25355519]
18. He J, Abdel-Wahab O, Nahas MK, Wang K, Rampal RK, Intlekofer AM, et al. Integrated genomic DNA/RNA profiling of hematologic malignancies in the clinical setting. Blood. 2016 Mar 10.
19. Cancer Genome Atlas Research N. Genomic and epigenomic landscapes of adult de novo acute myeloid leukemia. The New England journal of medicine. 2013 May 30; 368(22):2059–2074. [PubMed: 23634996]
20. Ding L, Ley TJ, Larson DE, Miller CA, Koboldt DC, Welch JS, et al. Clonal evolution in relapsed acute myeloid leukaemia revealed by whole-genome sequencing. Nature. 2012 Jan 26; 481(7382): 506–510. [PubMed: 22237025]
21. Ding L, Ellis MJ, Li S, Larson DE, Chen K, Wallis JW, et al. Genome remodelling in a basal-like breast cancer metastasis and xenograft. Nature. 2010 Apr 15; 464(7291):999–1005. [PubMed: 20393555]
22. Shlush LI, Zandi S, Mitchell A, Chen WC, Brandwein JM, Gupta V, et al. Identification of pre-leukaemic haematopoietic stem cells in acute leukaemia. Nature. 2014 Feb 20; 506(7488):328–333. [PubMed: 24522528]
23. McCormack E, Bruserud O, Gjertsen BT. Review: genetic models of acute myeloid leukaemia. Oncogene. 2008 Jun 19; 27(27):3765–3779. [PubMed: 18264136]
24. Xu D, Liu X, Yu WM, Meyerson HJ, Guo C, Gerson SL, et al. Non-lineage/stage-restricted effects of a gain-of-function mutation in tyrosine phosphatase Ptpn11 (Shp2) on malignant transformation of hematopoietic cells. The Journal of experimental medicine. 2011 Sep 26; 208(10):1977–1988. [PubMed: 21930766]
25. Welcker M, Clurman BE. FBW7 ubiquitin ligase: a tumour suppressor at the crossroads of cell division, growth and differentiation. Nature reviews Cancer. 2008 Feb; 8(2):83–93. [PubMed: 18094723]
26. Kats LM, Reschke M, Taulli R, Pozdnyakova O, Burgess K, Bhargava P, et al. Proto-oncogenic role of mutant IDH2 in leukemia initiation and maintenance. Cell stem cell. 2014 Mar 6; 14(3): 329–341. [PubMed: 24440599]
27. Distler E, Wolfel C, Kohler S, Nonn M, Kaus N, Schnurer E, et al. Acute myeloid leukemia (AML)-reactive cytotoxic T lymphocyte clones rapidly expanded from CD8(+) CD62L((high)+) T cells of healthy donors prevent AML engraftment in NOD/SCID IL2Rgamma(null) mice. Experimental hematology. 2008 Apr; 36(4):451–463. [PubMed: 18261837]
28. Majeti R, Chao MP, Alizadeh AA, Pang WW, Jaiswal S, Gibbs KD Jr, et al. CD47 is an adverse prognostic factor and therapeutic antibody target on human acute myeloid leukemia stem cells. Cell. 2009 Jul 23; 138(2):286–299. [PubMed: 19632179]
29. Taussig DC, Miraki-Moud F, Anjos-Afonso F, Pearce DJ, Allen K, Ridler C, et al. Anti-CD38 antibody-mediated clearance of human repopulating cells masks the heterogeneity of leukemia-initiating cells. Blood. 2008 Aug 1; 112(3):568–575. [PubMed: 18523148]

30. Mohi MG, Williams IR, Dearolf CR, Chan G, Kutok JL, Cohen S, et al. Prognostic, therapeutic, and mechanistic implications of a mouse model of leukemia evoked by Shp2 (PTPN11) mutations. Cancer cell. 2005 Feb; 7(2):179–191. [PubMed: 15710330]

31. Anderson K, Lutz C, van Delft FW, Bateman CM, Guo Y, Colman SM, et al. Genetic variegation of clonal architecture and propagating cells in leukaemia. Nature. 2011 Jan 20; 469(7330):356–361. [PubMed: 21160474]

32. Billerbeck E, Barry WT, Mu K, Dorner M, Rice CM, Ploss A. Development of human CD4+FoxP3+ regulatory T cells in human stem cell factor-, granulocyte-macrophage colony-stimulating factor-, and interleukin-3-expressing NOD-SCID IL2Rgamma(null) humanized mice. Blood. 2011 Mar 17; 117(11):3076–3086. [PubMed: 21252091]

33. Rongvaux A, Willinger T, Martinek J, Strowig T, Gearty SV, Teichmann LL, et al. Development and function of human innate immune cells in a humanized mouse model. Nature biotechnology. 2014 Apr; 32(4):364–372.

34. Pandey KR, Maden N, Poudel B, Pradhananga S, Sharma AK. The curation of genetic variants: difficulties and possible solutions. Genomics, proteomics & bioinformatics. 2012 Dec; 10(6):317–325.

35. Stein EM, Altman JK, Collins R, DeAngelo DJ, Fathi AT, Flinn I, et al. AG-221, an Oral, Selective, First-in-Class, Potent Inhibitor of the IDH2 Mutant Metabolic Enzyme, Induces Durable Remissions in a Phase I Study in Patients with IDH2 Mutation Positive Advanced Hematologic Malignancies. Blood. 2014 Dec 7. 2014; ASH abstract(115).

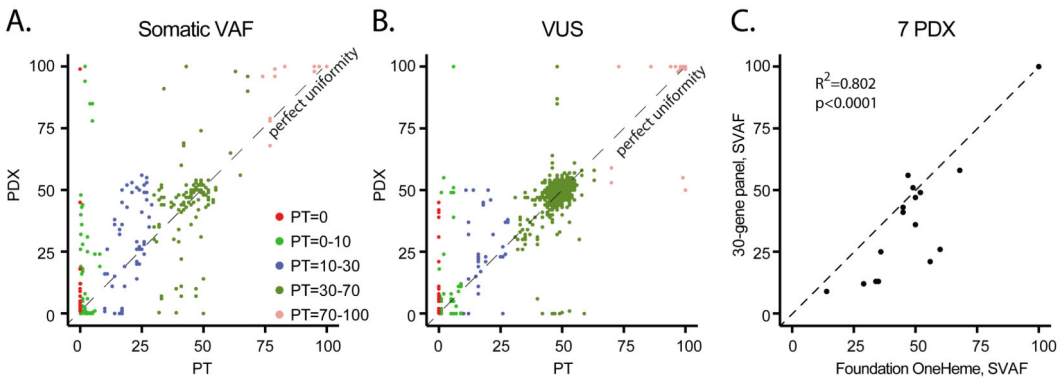


**Figure 1. Variant Allele Frequencies (VAF) correlate between patient and matched PDX samples**

Scatter plots of Somatic (S) VAF (**A**) and Variants of Unknown Significance (VUS) (**B**) between patient (PT) and patient-derived xenotransplant (PDX) samples. Colors represent VAF value ranges in PT samples as indicated (0; 0-10; 10-30; 30-70; 70-100). VAFs' correlations parameters within defined ranges are presented in sup table 6. **C.** Correlation of SVAF measured using FoundationOne Heme test and sequencing of amplicons of 30-genes

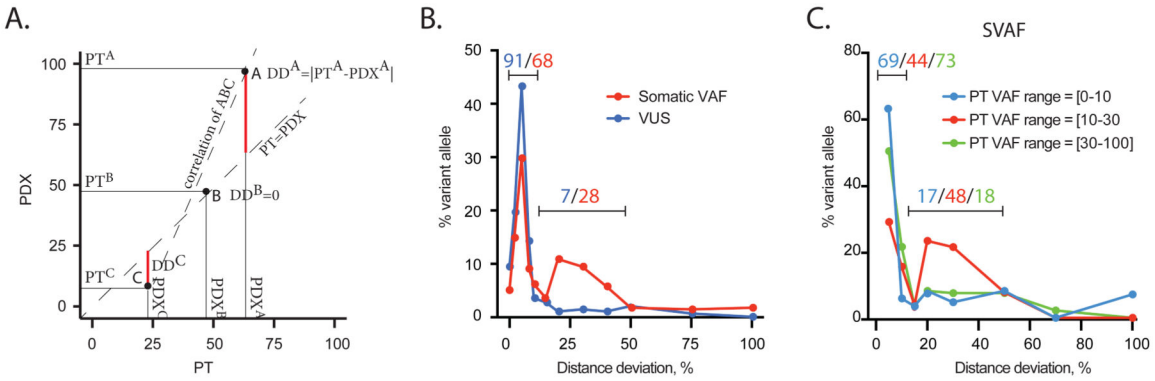


**Figure 2. Assessment of variability of somatic VAFs**

**A**. Rational for calculation of distance deviation (DD) for VAF. Suppose, VAF"A", "B" and "C" correlate forming "correlation ABC" dotted line. However, this correlation does not account enrichment of clone marked with VA "A" and loss of clone marked with VA "C". Therefore, we derived a DD metric, calculated as absolute difference between PT and PDX VAF values, that reflects distribution of VAF. The smaller DD the closer SVAF is located to PT=PDX line. Higher DD is a measure of higher variability. **B.** Histogram representation of DD distribution of 274 SVAFs (red) and 714 VUSs (blue). 91% of VUSs have a DD<10%, where as only 68% of SVAFs have a DD<10%; 28% of SVAFs and 7% VUS have a DD in the 15-50% range. **C.** Histogram representation of DD distribution in different SVAF value ranges in PT samples. 0-10% and 30-100% ranges have >68% DD values<10%; while 10-30 range has only 44% DD values <10%. Both, 0-10% and 30-100% ranges have <20% DD in 15-50% range, while 10-30 range has >48% DD in 15-50% range. Higher DD means higher variability.

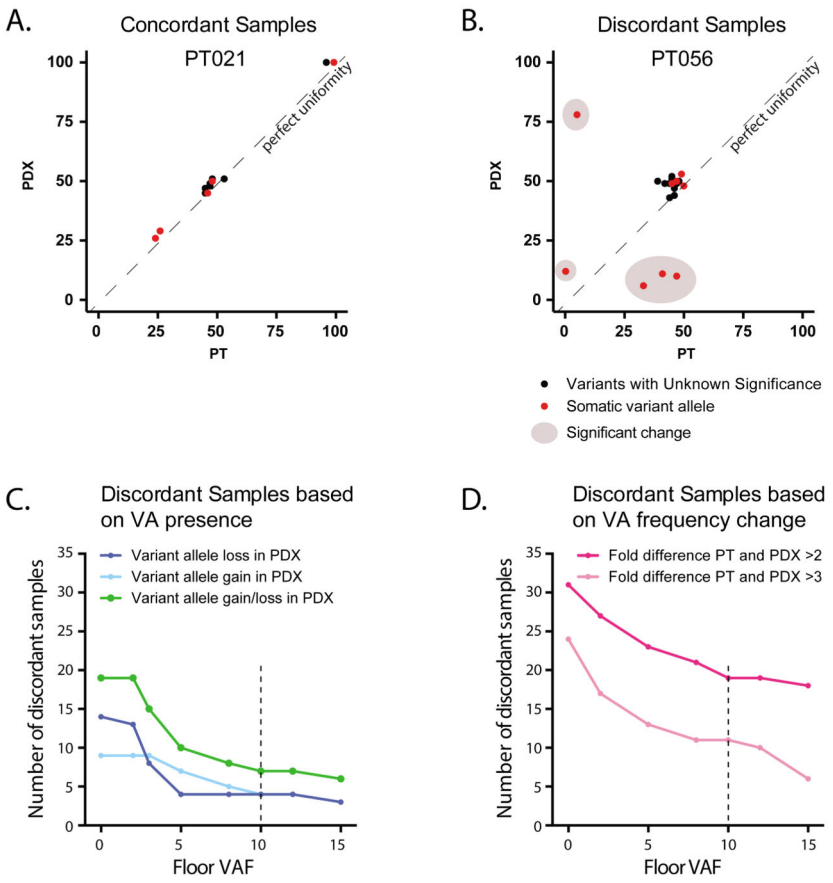


**Figure 3. Correlation of SVAFs and VUSs in individual PT-PDX pairs**

Examples of concordant (**A**) and discordant (**B**) PT-PDX pairs based on SVAF and VUS distribution visualized as scatter plots. Clustering of SVAF closer to “perfect uniformity” (PT=PDX) lines indicates concordance. The number of discordant samples was calculated on the basis of the presence or absence of somatic variant alleles (**C**) or the fold change in SVAF between PT and PDX samples (**D**) using a sliding window SVAF floor from 0 to 15.

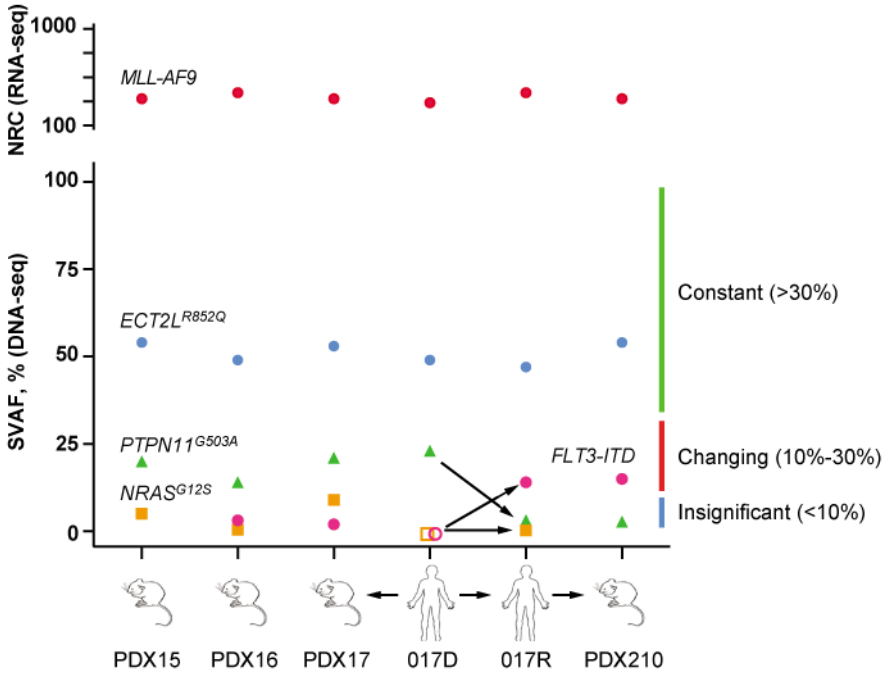


**Figure 4. PDX samples broadly represent clonal architecture of PT samples**

Targeted sequencing of diagnostic (D) PT sample revealed 3 SVAF: *MLL-AF9* filled red circles, *ECT2L*$^{R852Q}$ filled blue circles, and *PTPN11*$^{G503A}$, filled green triangle. 3 PDX samples originated from 017D had an additional *NRAS*$^{G12S}$ (filled orange squares); 2 PDX samples had an additional *FLT3-ITD* (filled purple circles). We hypothesized that 017D had these two additional SVAF under detection limit (empty circle and square). Targeted sequencing of 017 relapse (R) identified all 5 alleles *MLL-AF9*, *ECT2L*$^{R852Q}$, *PTPN11*$^{G503A}$, *NRAS*$^{G12S}$, and *FLT3-ITD*. It is likely that 2 clones uniquely marked with *PTPN11*$^{G503A}$ and *FLT3-ITD* changed their frequencies. The clone marked with *NRAS*$^{G12S}$ was a minor clone and remained a minor clone. While *PTPN11*$^{G503A}$ and *FLT3-ITD* alleles were changing frequencies and NRAS$^{G12S}$ allele was always <10%, MLL-AF9 and ECT2L$^{R852Q}$ alleles did not change frequency.

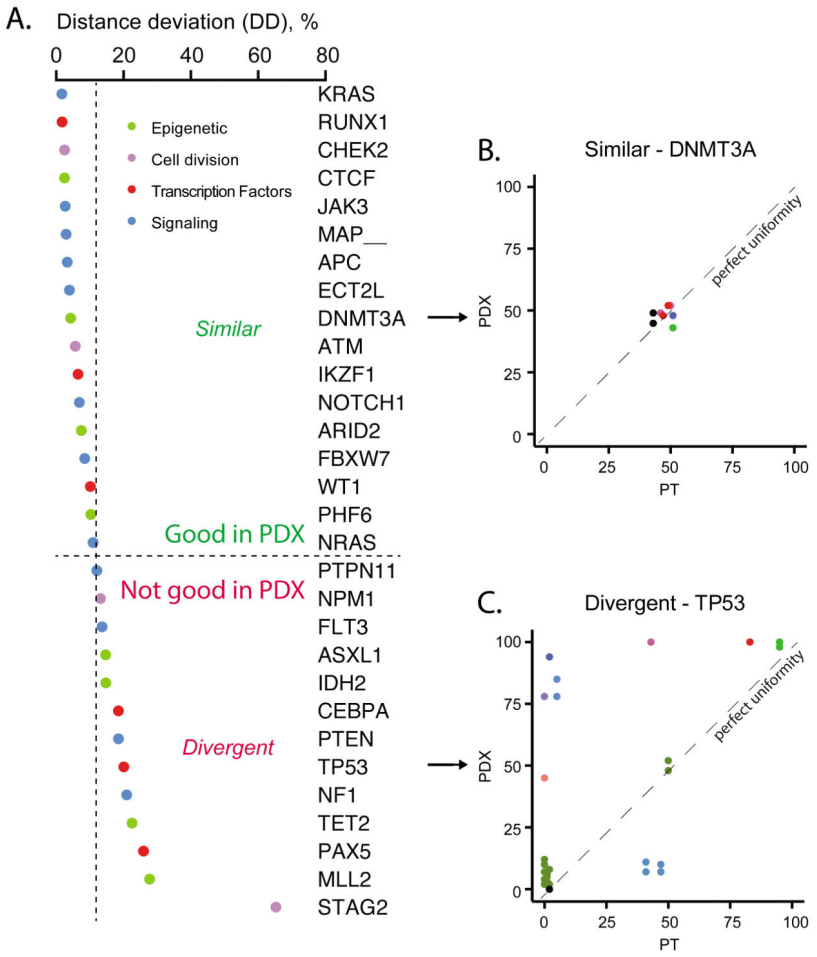


**Figure 5. Correlation of SVAF of specific genes in PT-PDX pairs**

**A.** 30 recurrently mutated genes were ranked on the basis of SVAF distance deviation (DD), calculated as in figure 2A. Colors represent commonly annotated gene classes/functions. Mean DD (12.7%) was used as a threshold dividing similarly and divergently engrafting alleles, data presented in sup table 10. Scatter plot presentation of examples for *similar* (**B**) and *divergent* (**C**) variant alleles in PT and PDX pairs. Alleles with similar frequencies cluster around the “perfect uniformity” line. SVAF are color-coded per unique PT samples.

*Leukemia*. Author manuscript; available in PMC 2017 January 06.

**Table 1**

**Engraftment of PT samples into NSG mice**

Classification of 160 transplanted PT samples by lineage and type of the disease: “All” – samples transplanted per lineage; “New” – new diagnosis; “Rel” – relapsed; “Ref” – refractory; “Ther” – therapy related; “N/A”– data not available. Classification of patients: “Ped” – patients treated by the pediatric department on pediatric protocols, or age 0-18; “Adult” –patients treated by the department of adult medicine, or>18 years. Engraftment: “Any” – engraftment of any human immunophenotype; “Correct” the expected lineage of human cells were detected in mouse bone marrow. Engraftment level: percent of transplanted mice that engrafted with PT samples. 83 (70%)and 24 (20%) PT samples engrafted in 100% and 50% of transplanted mice with correct lineage, respectively.

| | | Disease classification | | | | | Patient age | | | Engraftment | | Engraftment level | | | |
|---|---|---|---|---|---|---|---|---|---|---|---|---|---|---|---|
| **Disease** | **All** | **New** | **Rel** | **Ref** | **Ther** | **N/A** | **Ped** | **Adult** | **N/A** | **Any** | **Correct** | **100%** | **67%** | **50%** | **33%** |
| AML | 56 | 25 | 19 | 9 | 2 | 1 | 8 | 48 | | 48 | 45 | 24 | 7 | 9 | 5 |
| MLL | 2 | 1 | 1 | | | | 1 | 1 | | 2 | 2 | 1 | | 1 | |
| B-ALL | 32 | 15 | 15 | 2 | | | 10 | 22 | | 25 | 24 | 15 | | 9 | |
| T-ALL | 70 | 42 | 4 | | | 24 | 32 | 33 | 5 | 48 | 48 | 43 | | 5 | |
| Total: | 160 | 83 | 39 | 11 | 2 | 25 | 51 | 104 | 5 | 123 | 119 | 83 | 7 | 24 | 5 |
| | | | | | | | | | | | | 70% | | 20% | |

**Table 2**

**Leukemia lineage specific distribution of recurrent genetic variants detected by FoundationOne Heme test**

Detection of short nucleotide variances (SNV); copy number alterations (CNA); and known or likely (computationally predicted in frame) chromosomal rearrangements (RE) in 18 AML, 23 B-ALL, 2 MLL, and 24 T-ALL PT and PDX samples, across 4 leukemia lineages. “PT” - number of primary tumor (PT) samples in which a lesion was detected.

| | Types of genetic lesions | | | | | Diseases | | | |
|---|---|---|---|---|---|---|---|---|---|
| **Gene** | **PT** | **SNV** | **CNA** | **RE, known** | **RE, likely** | **AML** | **MLL** | **B-ALL** | **T-ALL** |
| *CDKN2A* | 28 | | 28 | | | | | 7 | 21 |
| *CDKN2B* | 22 | | 22 | | | | | 6 | 16 |
| *TP53* | 12 | 12 | | | | 3 | | 7 | 2 |
| *MLL1* | 12 | 1 | | 11 | | 6 | 1 | 4 | 1 |
| *FLT3 (inc. ITD)* | 11 | 11 | | | | 8 | | 2 | 1 |
| *NOTCH1* | 11 | 11 | | | | | | 1 | 10 |
| *WT1* | 11 | 11 | | | | 5 | | | 6 |
| *NRAS* | 10 | 10 | | | | 1 | | 4 | 5 |
| *PTEN* | 10 | 8 | 2 | | | | | 1 | 9 |
| *PTPN11* | 9 | 9 | | | | 5 | | 2 | 2 |
| *NPM1* | 7 | 7 | | | | 7 | | | |
| *JAK1/2/3* | 6 | 6 | | | | 1 | | 2 | 3 |
| *PAX5* | 6 | 2 | 1 | | 3 | | 1 | 5 | |
| *DNMT3A* | 6 | 6 | | | | 4 | | | 2 |
| *KRAS* | 6 | 6 | | | | 2 | | 3 | 1 |
| *ASXL1* | 5 | 5 | | | | 3 | | 1 | 1 |
| *IDH1/2* | 5 | 5 | | | | 5 | | | |
| *ETV6* | 5 | 2 | 2 | 1 | | | | 4 | 1 |
| *RUNX1* | 5 | 3 | | | 2 | 4 | | | 1 |
| *TET2* | 4 | 3 | 1 | | | 3 | | 1 | |
| *CEBPA* | 4 | 4 | | | | 4 | | | |
| *FBXW7* | 4 | 4 | | | | | | 2 | 2 |
| *MLL2* | 4 | 4 | | | | | | 2 | 2 |
| *TCF3* | 4 | 1 | | 1 | 2 | 1 | 1 | 1 | 1 |

| | Types of genetic lesions | | | | | Diseases | | | |
|---|---|---|---|---|---|---|---|---|---|
| **Gene** | **PT** | **SNV** | **CNA** | **RE, known** | **RE, likely** | **AML** | **MLL** | **B-ALL** | **T-ALL** |
| *RB1* | 4 | 2 | 1 | | 1 | | | 3 | 1 |
| *APC* | 3 | 3 | | | | | | | 3 |
| *NF1* | 3 | 3 | | | | 2 | | 1 | |
| *PHF6* | 3 | 3 | | | | | | 1 | 2 |
| *IKZF1* | 3 | 3 | | | | | | 1 | 2 |
| *ATM* | 2 | 2 | | | | | 1 | | 1 |
| *CREBBP* | 2 | 2 | | | | 1 | | 1 | |
| *EP300* | 2 | 2 | | | | | | 2 | |
| *U2AF1* | 2 | 2 | | | | 1 | | | 1 |
| *CRLF2* | 2 | | | 2 | | | | 2 | |
| *PBX1* | 2 | | | 2 | | | 1 | 1 | |
| *MYH11* | 2 | | | 2 | | 2 | | | |